Journal Pre-proofs

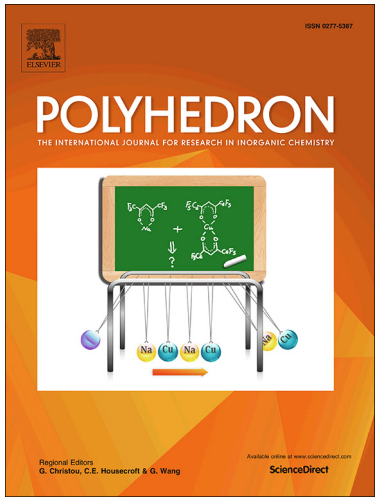

Synthesis, characterization and in vitro evaluation of anticancer activity of a new water-soluble thiosemicarbazone ligand and its complexes

Soheila Jenabi Sardroud, Seyed Abolfazl Hosseini-Yazdi, Majid Mahdavi, Morgane Poupon, Eliska Skorepova

PII: S0277-5387(19)30663-1
DOI: https://doi.org/10.1016/j.poly.2019.114218
Reference: POLY 114218

To appear in: *Polyhedron*

Received Date: 29 June 2019
Revised Date: 24 October 2019
Accepted Date: 25 October 2019

Please cite this article as: S.J. Sardroud, S.A. Hosseini-Yazdi, M. Mahdavi, M. Poupon, E. Skorepova, Synthesis, characterization and in vitro evaluation of anticancer activity of a new water-soluble thiosemicarbazone ligand and its complexes, *Polyhedron* (2019), doi: https://doi.org/10.1016/j.poly.2019.114218

Synthesis, characterization and in vitro evaluation of anticancer activity of a new water-soluble thiosemicarbazone ligand and its complexes

Soheila Jenabi Sardroud[a], Seyed Abolfazl Hosseini-Yazdi[a,*], Majid Mahdavi[b], Morgane Poupon[c], Eliska Skorepova[c]

[a]Department of Inorganic Chemistry, Faculty of Chemistry, University of Tabriz, Tabriz 51666-14766, Iran

[b]Department of Biology, Faculty of Natural Sciences, University of Tabriz, Tabriz, Iran

[c]Institute of Physics of the Czech Academy of Sciences, Na Slovance 2, 182 21 Prague 8, Czech Republic

*Corresponding author: Department of Inorganic Chemistry, Faculty of Chemistry, University of Tabriz, Tabriz 51666-14766 Iran. Seyed Abolfazl Hosseini-Yazdi (hosseiniyazdi@tabrizu.ac.ir.com , hosseiniyazdi@yahoo.com)

Tel.:+98-4133393134, fax: +98-4133340191

Abstract

A new water-soluble thiosemicarbazone ligand, 4-hydroxyl-3-({[(methylamino)carbonothioyl] hydrazono}methyl)benzoic acid (**H_3L^{COOH}**) and its complexes with Cu(II), Ni(II), Zn(II), Fe(III) and Mn(III) were synthesized and characterized. These compounds were characterized by conductivity, magnetic susceptibility, elemental analysis, FT-IR, ^{1}H NMR, ^{13}C NMR, and UV-Vis spectroscopy. All the compounds have sufficient solubility and stability in water as a safe, green, and biologic solvent. The compounds were evaluated for their anticancer activities against the human chronic myelogenous K562 leukemia and human breast carcinoma MCF-7 cell lines. All the complexes significantly showed more anticancer activity than the ligand alone and the Cu(II) complex showed considerable cytotoxicity against the tested cell lines. The mechanism of action of the most potent complex, **Cu(HL^{COO})** against K562 cell line was further explored by fluorescence microscopy, flow cytometry, cell cycle and reactive oxygen species (ROS) assays. Hoechst staining and flow cytometry indicated the apoptosis induction ability of **Cu(HL^{COO})** on K562 cells. Mechanistic studies indicated that **Cu(HL^{COO})** complex caused cell cycle arrest at G0/G1 phase and this complex was able to inhibit the cell cycle in a time-dependent manner. **Cu(HL^{COO})** can also increase the reactive oxygen species levels in the K562 cells. The obtained results suggest that the studied compounds can be helpful candidates for further evaluations as chemotherapeutic agents in the treatment of cancer.

Keywords: Apoptosis; Cell cycle; Cytotoxicity; Flow cytometry; Schiff base; Thiosemicarbazone

1. Introduction

Nowadays cancer is considered to be a threatening illness and also a top trend in the field of therapeutic chemistry. Chemotherapy with metal complexes is an effective approach for fighting against cancer. For example, Cisplatin is an efficient anticancer drug for treating various tumours, but it causes some problems due to its resistance and critical side effects [1, 2]. Hence, continual studies are going on to develop other antitumour-active inorganic complexes to conquer these problems [3-7]. Thiosemicarbazone metal complexes have been interesting for researchers because of having various biological activities such as antiviral [8], antibacterial, [9-11] and anticancer [12-17] activities. These compounds have shown selective and noticeable antitumour activites and conquering the persistence to chemotherapy [18-24]. For studying the biological activity of the metal complexes, it is important to provide natural biological conditions and insolubility of the metal complexes in water has been a disadvantage. So it is of great importance to design new thiosemicarbazone chelators and developing new metal complexes with them in order to highten their water solubility character to be studied in the field of cancer treatment [25]. Most of the water soluble ligands have hydrophilic groups such as carboxylate or sulfonate moieties [26]. Recently we have introduced the sulfonate group as a part of thiosemicarbazones ($H_2L^{SO_3^-}$) for increasing the water solubility character (Scheme 1) [27]. Water solubility of the complexes was metal-dependent and anticancer activity of the complexes and ligands was studied on some leukemia cell lines. Effect of the substituents on the ligands and the type of metal were investigated on activity of the complexes. Therefore, in this paper we introduced carboxylate group to increase aqueous solubility of also the ligand and evaluated the effect of carboxylate group on solubility, stability, and anticancer activity on the MCF-7 and K562 cell lines. More over, in this work we improved depth of anticancer study of the compounds with flow cytometry, cell cycle and ROS assays.

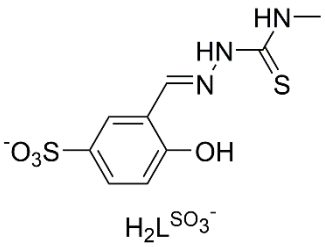

Scheme 1. Structure of the ligand $H_2L^{SO_3^-}$

2. Experimental section

2.1. Materials and instrumentation

The reagents and chemicals used in the present study were bought were purchased from commercial sources and used without purification. 3-(4, 5-Dimathylthiazol-2-yl)-2,5-diphenyltetrazolium bromide (MTT) was bought from Sigma-Aldrich company. Fetal bovine serum (FBS) was purchased from HyClone. RPMI 1640 was bought from Gibco. The human K562 and MCF-7 cell lines were obtained from Pasteur Institute (Tehran, Iran). Annexin-V FITC apoptosis kit, propidium iodide (PI), and cell extraction buffer were bought from Invitrogen (United States). The ^{1}H NMR and ^{13}C NMR spectra were studied on a Bruker Avance 400 spectrometer in d_6-DMSO. UV–Vis measurements were performed with a Shimadzu UV–Vis 1700 spectrophotometer in H_2O and DMSO. Using KBr pellets, infrared spectra were recorded on an FTIR Bruker Tensor 27 spectrometer. C, H, N, and S analyses were done on an Elementar Vario El III Melting points were measured with an Electrothermal 9300. Magnetic susceptibility were determined by Evans NMR method in d_6-DMSO and TMS as a reference material [28]. Molar conductivity were measured using a cond 7110 WTW conductometer.

2.2. Synthesis of 3-formyl-4-hydroxybenzoic acid

3-Formyl-4hydroxybenzoic acid synthesised as stated by the literature [29] with slight modification (Scheme 2). 4-hydroxylbenzoic acid (22 mmol, 3.0 g) suspended in 10 mL trifluoroacetic acid (TFA) was added drop-wise to hexamethylenetetramine (22 mmol, 3.1 g) dissolved in trifluoroacetic acid and was refluxed by heating under argon atmosphere for 2 h. When cooled, the obtained solution was stirred using 4 M HCl (300 mL) for 3 h. The yellowish powder was collected and washed with an excess of brine. Then it was dissolved in ether and dried. Yield: 3.5 g (19%). ^{1}H NMR (DMSO- d_6): δ 12.86 (s, 1H, COOH), 11.47 (s, 1H, ArOH), 10.29 (s, 1H, CHO), 8.23 (d, 1H, ArH), 8.04 (dd, 1H, ArH), 7.07 (d, 1H, ArH).

2.3. Synthesis of 4-hydroxyl-3-({[(methylamino)carbonythioyl] hydrazono} methyl) benzoic acid (H_3L^{COOH})

3-Formyl-4-hydroxy-benzoic acid (6.01 mmol, 1.0 g) was dissolved in MeOH (50 mL) and refluxed by heating gradually. A solution of 4-methyl-3-thiosemicarbazide in methanol (6.01 mmol, 0.63 g) was added to the above solution, then the obtained solution was refluxed for 3 h. By cooling and evaporating the solvent at room temperature, the ligand was formed as a yellow precipitation (Scheme 2). Yield: 1.5 g (98%). Sample decomposes above 300 °C. ^{1}H NMR (d_6-DMSO): δ 12.65 (broad s, 1H, COOH), 11.46 (s, 1H, ArOH), 10.75 (broad s, 1H, NH), 8.47 (quartet, 1H, NH), 8.44 (d, 1H, ArH), 8.39 (s, 1H, ArCHN), 7.79 (dd, 1H, ArH), 6.94 (d, 1H, ArH), 3.01 (d, 3H, CH_3) ppm. ^{13}C NMR (d_6-DMSO): δ 177.6 (C=S), 167.1 (COOH), 160.1 (CH=N), 138.6 (Ar), 132.3 (Ar), 128.3 (Ar), 122.1 (Ar), 120.5 (Ar), 115.9 (Ar), 31.0 (CH_3). Selected FT IR data (KBr disc, cm^{-1}): 3438 s, 3344 s, 3136 s, 2938 m, 1670 s (C=O), 1651 s, 1536 s, 1489 s, 1443 s, 1280 s, 763 m, 625 s, 532 m.

2.4. Synthesis procedures of the complexes

A methanol solution of the $Mn(CH_3COO)_3.2H_2O$, $FeCl_3$, $Ni(CH_3COO)_2.4H_2O$, $Cu(CH_3COO)_2.H_2O$ and $Zn(CH_3COO)_2.2H_2O$ (1 mmol) was added drop-wise to the solution containing the ligand in methanol (1 mmol) and stirred for 4 h. The obtained precipitate was filtered off and washed with cold methanol.

Mn(HL^{COO})(OAc). Brown precipitate, Yield: 0.27 g (64%). Anal. Calc. (%) for $Mn(HL^{COO})(OAc)\cdot 3H_2O$ ($C_{12}H_{18}MnN_3O_8S$; F.W.= 419.291) C 34.37, H 4.33, N 10.02, S 7.65; Found (%): C 34.08, H 3.98, N 9.78, S 7.36. Selected FT IR data (KBr disc, cm^{-1}): 3407 s, 2930 m, 1610 s, 1552 s, 1489 s, 1377 s, 1275 s, 677 m.

Fe(HL^{COO})Cl. Dark brown precipitate, Yield: 0.30 g (83%). Anal. Calc. (%). For $Fe(HL^{COO})Cl\cdot H_2O$ ($C_{10}H_{11}ClFeN_3O_4S$; F.W.= 360.576) C 33.31, H 3.07, N 11.65, S 8.89; Found (%): C 33.04, H 2.83, N 11.32, S 8.73. Selected FT IR data (KBr disc, cm^{-1}): 3435 m, 1697 s (C=O), 1640 s, 1520 s, 1480 s, 1466 s, 1273 s, 672 m.

Ni(HL^{COO}). Brown precipitate, Yield: 0.28 g (85%). Anal. Calc. (%) for $Ni(HL^{COO})\cdot H_2O$ ($C_{10}H_{11}NiN_3O_4S$; F.W.= 327.972) C 36.62, H 3.38, N 12.81, S 9.78; Found (%): C 36.18, H 3.01, N 12.38, S 9.46. Selected FT IR data (KBr disc, cm^{-1}): 3437 m, 2928 m, 1693 s (C=O), 1609 s, 1593 s, 1543 s, 1203 s, 670 s, 514 m.

Cu(HL^{COO}). Green precipitate, Yield: 0.22 g (66%). Anal. Calc. (%). for $CuHL^{COO}\cdot H_2O$ ($C_{10}H_{11}CuN_3O_4S$; F.W.= 332.824) C 36.09, H 3.33, N 12.63, S 9.63; Found (%): C 36.24, H 3.04, N 12.42, S 9.56. Selected FT IR data (KBr disc, cm^{-1}): 3397 s, 2859 m, 1689 s (C=O), 1602 s, 1515 s, 1404 s, 1269 s, 670 s, 535 m.

Zn(HL^{COO}). Yellow precipitate, Yield: 0.31 g (88%). Anal. Calc. (%). For $Zn(HL^{COO})\cdot 2H_2O$ ($C_{10}H_{13}N_3O_5SZn$; F.W= 352.683) C 34.06, H 3.72, N 11.91, S 9.09; Found (%): C 33.52, H 3.64,

N 11.59, S 8.89. ^{1}H NMR (DMSO-d_6): δ 8.35 (s, 1H, CHN), 7.81 (s, 1H, ArH), 7.63 (d, 1H, ArH), 6.67 (s, 1H, ArH), 2.77 (s, 3H, CH_3). Selected FT IR data (KBr disc, cm^{-1}): 3221 m, 2869 m, 1618 s, 1518 s, 1485 s, 1377 s, 1270 s, 685 s, 505 m.

2.5. Single crystal X-ray diffraction studies

Crystallographic studies were performed with a four-circle CCD diffractometer at 120 K, Gemini of Oxford Diffraction, using Cu/K_α radiation (λ = 1.54184 Å) radiated from a classical sealed tube monochromated by using graphite and collimated by fibre-optics Enhance collimator. A CCD detector was also utilized. Cell refinement, data collection, and reduction, and absorbance corrections performed using CrysAlisPro 1.171.39.35 [30]. By means of equivalent radius and absorption coefficient the spherical absorption correction was done. The recorded crystal was twinned with the twin law of 180° around c-axis with a ratio per domains 62/38 %. Charge flipping method using Superflip was used to solve the structure which was refined by least-squares calculations on F^2 with Jana2006 [31, 32]. Difference Fourier maps were studied to descen the hydrogen atoms in the structure. H atoms which were bonded to C atom were in their ideal position (C-H bond, 0.96 A°). But those were bonded to N were refined in a new geometry. In this survey, U_{iso} (H) was fixed to 1.2 times of U_{eq} of C, N, and O. The other atoms (except hydrogen) were refined using harmonic refinement.

2.6. Lipophilicity measurement

A shake-flask method was performed to determine the lipophilicity of the compounds [33]. 50 mL of 1-octanol and 50 mL of water were mixed and shaken for 24 h for saturation of both phases. An aqueous solution containing 5 µM of the synthesised compounds were prepared. Consequently 3

mL of the prepared solutions were added to 3 mL of 1-octanol. The obtained solutions were shaken for a night and then centrifuged for the separation of the two phases. Finally the concentration of the target compounds were analysed before and after mixing with 1-octanol using a UV-Vis spectrophotometry.

2.7. Cell culture

MCF-7 (human breast carcinoma cell line) and K562 (human chronic myelogenous leukemia) cells were obtained from National Cell Bank of Iran (Pasteur Institute, Tehran, Iran). The cells were grown in RPMI-1640 medium supplemented with 10% fetal bovine serum (FBS) (Sigma), 100 U/mL penicillin and 100 mg/mL streptomycin (Sigma) and subsequently were incubated in a humidified incubator containing 5% CO_2 at 37 °C.

2.8. MTT assay

The cytotoxic effect of the compounds was assessed against human cancer cell lines (K562 and MCF-7) by utilizing the 3-(4,5-dimethylthiazol-2-yl)-2,5-diphenyltetrazoliumbromide (MTT) assay according to the manufacturer's protocol [34, 35]. The procedure is on the basis of the reduction of MTT by the mitochondrial dehydrogenases to the crystals of formazan. Cells (1×10^5 cells/well) were seeded into 96 well plates and treated with different concentrations of the compounds for 24 and 48 h. After the treatment, 20 µL of the MTT solution (5 mg/mL in PBS) were added to each well and incubation was continued for 4 h. The purple-blue MTT formazan precipitate was dissolved in 200 µL of DMSO and the absorbance values at 570 nm were measured on a multiwall plate reader (Quant Bio-tek Instruments, Winooski, VT, USA). Untreated K562 and MCF-7 cells were used as a negative control. The cytotoxity effect of Doxorubicin and Paclitaxel drugs were examined against K562 and MCF-7 cells, respectively, as positive control. The performed experiments were repeated three times.

2.9. Morphological evaluation of the apoptotic cells

Apoptosis induction was examined using Hoechst staining (blue fluorescent dye), which intercalate with DNA. The K562 cells were cultured in 12 well plates and treated with IC_{50} dose of **Cu(HL^{COO})** (as the most potent complex) for 48 h at 37 °C in a humidified 5% CO_2 atmosphere. Finally, after washing the cells with PBS, DNA was stained with Hoechst 33258 (1 mg/mL) in PBS for 5 min and evaluated by fluorescence microscopy (Olympus BX41, Germany).

2.10. Apoptosis survey using by Flow Cytometric Analysis

The annexin-V and PI (propidium iodide) dyes were used to differentiate between necrotic and apoptoic cells. According to the manufacture's protocol, an annexin-V FITC/PI double staining method was utilized. Briefly, K562 cells were cultivated after the treatment with **Cu(HL^{COO})** complex. The elusion of treated and untreated cells was performed with PBS for two times. Then 1×10^6 cells were resuspended in binding buffer (10 mM HEPES/NaOH, pH 7.4, 140 mM NaCl, 2.5 mM $CaCl_2$). Then, 5 µL of PI and 5 µL of annexin-V FITC were added. The obtained solution was incubated in the dark place at room temperature for 15 min. Finally it was analysed by flow cytometry (BD FACSCalibur flow cytometer, USA).

2.11. Analysis of cell cycle

In order to investigate the cell cycle phase distribution of K562 cells in response to the **Cu(HL^{COO})** complex the DNA content of cells was analysed. For this analysis, the cells (5×10^4 cell/well) were seeded in 6-well plates 24 h prior to treatment. The treated cells with a single dose (at IC_{50} value) of the complex were collected after 24 and 48 h, and eluted for 2 times with PBS. After that, cells were harvested, fixed in 70% ethanol and kept at -20 °C overnight. Then the cells were stained with a solution containing 1% Triton-X 100 in PBS, treated with RNase (20 µg/mL) and exposed to the DNA binding dye propidium iodide (50 µg/mL) for 30 min in darkness. The samples were

then analysed with a flow cytometer (BD FACSCalibur flow cytometer, USA) and the percent of calculated cells in the sub-G1, G0/G1, S, and G2/M phases were determined.

2.12. Intracellular ROS measurements

Reactive oxygen species (ROS) have a significant role in apoptosis induction in the pathologic conditions and physiologic [36, 37]. The amount of ROS present in cells treated with **Cu(HL^{COO})** was analysed using 2′,7′-dichloro-dihydro-fluorescin diacetate (DCFH-DA). The dye is deacetylated to a non-fluorescent compound, by cellular esterases after diffusion into the cell which is susequently oxidized by ROS into 2',7'-dichlorofluorescein (DCF). DCF is a fluorescent chemical with maximum excitation and emission spectra of 495 and 529 nm, respectively. Thus, the fluorescence intensity is dependent to the amount of peroxide generated by the cells. DCFH-DA with a concentration of 10 µM, was added to the cell medium 30 min before the end of the treatment. The cells were collected by centrifugation at 2000 rpm for 5 min at 4 °C, eluted for two times with PBS to eliminate the extracellular compounds, and DCFH-DA fluorescence was detected using flow cytometry (BD FACSCalibur, USA).

3. Results and discussion

3.1. Synthesis and characterization

The ligand was obtained by the condensation of 3-formyl-4-hydroxy-benzoic acid and 4-methyl thiosemicarbazide (Scheme 2) and characterized by FTIR, ^{1}H NMR, ^{13}C NMR, CHN analysis and single-crystal X-ray diffraction. Elemental analysis, ^{1}H NMR and ^{13}C NMR showed that the ligand has high purity without any excess peaks corresponding to starting materials or an unflavoured product. Singlet peak corresponding to the aldehyde proton at 10.29 ppm in 3-formyl-4-hydroxy-benzoic acid completely disappeared and a singlet peak at 8.38 ppm was found corresponding to the iminic proton. Peaks of the protons of COOH and NH-N groups were found as broad singlets at 12.64 and 10.75 ppm, respectively. In ^{13}C NMR, 10 peaks were found corresponding to the expected structure. The FTIR spectrum of KBr disc of the ligand showed a strong absorption band at 1651 cm^{-1} corresponding to C=N stretching vibration after condensation of aldehyde and 4-methyl thiosemicarbazide. In the FTIR spectrum of the ligand, a strong band corresponding to C=O stretching vibration of COOH group was found at 1670 cm^{-1}.

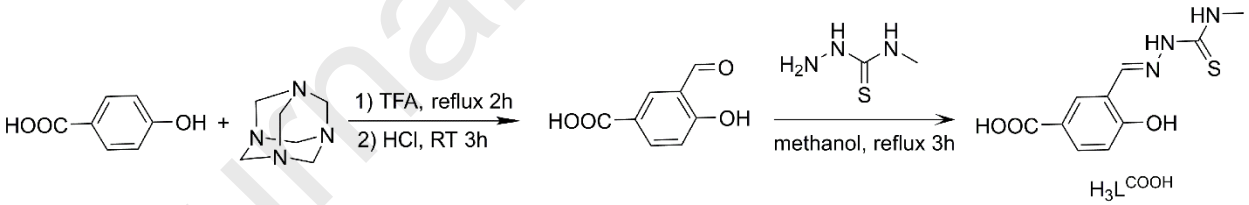

Scheme 2: Synthetic pathways for aldehyde and the ligand

The complexes were produced by the reaction between the ligand and metal salts in methanol in reflux. All complexes are stable on air. The complexes are soluble in methanol, DMF, DMSO, and water. Solubilities for **H_3L^{COOH}**, **Mn(HL^{COO})(OAc)**, **Fe(HL^{COO})Cl**, **Ni(HL^{COO})**, **Cu(HL^{COO})** and **Zn(HL^{COO})** in water are 40, 2.4, 2.2, 4, 3 and 2.6 g/L, respectively. Unfortunately, all endeavours to achieve a single crystal of complexes were unsuccessful. So, it was very difficult for us to assign

exact structures for the complexes. However, we have proposed legal structures for complexes by using elemental analysis, FT-IR, ^{1}HNMR, molar conductivity, magnetic susceptibility and electronic absorption spectroscopy methods and refer to previous our research in this field [27, 38, 39].

In the FT-IR spectrum of **Cu(HL^{COO})** complex a strong band corresponding to C=O appeared at 1689 cm^{-1} higher than 1670 cm^{-1} in the free ligand, **H$_3$L^{COOH}**. So, carboxylate group of the ligand has been coordinated to metal center as a unidentate mode [40]. The measured magnetic moment of the compound in DMSO by Evaus method was found to be 1.93 BM. The complex exhibits a broad band from about 500 to 800 nm with a maximum at 518 nm corresponding to a four-coordinate square planar geometry (Fig. 1a) which is strongly favorable for the d^9 configuration [41]. Also, 10^{-3} M solution of this complex in DMSO is nonelectrolyte. On the other hand, our recent research with the similar ligand with sulfonate group have showed the coordination of sulfonate group to the metal center and forming dinuclear complexes [27, 38, 39]. All in all, we can propose structure shown in Fig. 2 for this complex.

Mn(HL^{COO})(OAc) complex shows no signal above 1610 cm^{-1} in the region of carbonyl group in FT-IR spectrum. So, in this complex carboxylate group of the ligand and acetate group should be coordinated to Mn(III) as a chelating or ionic. We think acetate anion is coordinated to metal as a chelating bidentate ligand because this complex is nonelectrolyte in solution. So acetate anion remains coordinated in solution. On the other hand, after coordination of the ligand as three-dentate and acetate anion as bidentate, coordination of carboxylate group as a chelating ligand to the metal center is difficult to form seven-coordinate complex. However coordination of H_2O to Mn(III) in order to from a octahedral structure is possible. Magnetic moment of the complex in DMSO is 4.23 BM, corresponding to a d^4 high spin complex. Overall, our proposed structure for

Mn(HL^{COO})(OAc) is shown in the Fig. 2. Manganese(III) six-coordinate complexes commonly cause to form fairly intense ligand field bands [41]. This probably originates from a coordination of factors such as; a fairly covalent metal ligand band, low symmetry components to the ligand field, and fairly low lying CT bands [41]. As a result we can not see a separated band for this complex because of the above mentioned reasons (Fig. 1).

In the FT-IR spectrum of **Fe(HL^{COO})Cl**, a strong band at 1697 cm^{-1} is seen which is corresponding to unidentate coordination mode of carboxylate group in the solid state. Magnetic moment of the complex is 5.20 BM in agreement with a d^5 high spin configuration in DMSO solution. Also, molar conductivity (Λ_m = 20 $cm^{-1}mol^{-1}\Omega^{-1}$) is lower than a 1:1 electrolyte solutions [42] namely chloride anion partially separated in DMSO. In electronic absorption spectrum of the complex only a shoulder can be seen around 500 nm (high energy) related to a ligand to metal charge transfer transition (Fig. 1a). Overall, based on all data a dinuclear structure in octahedral geometry is proposed for **Fe(HL^{COO})Cl** complex (Fig. 2).

In the FT-IR spectrum of the **Ni(HL^{COO})** complex, a band corresponding to C=O is appeared at 1693 cm^{-1} higher than 1670 cm^{-1} for **H_3L^{COOH}**. Therefore, similar to **Cu(HL^{COO})** and **Fe(HL^{COO})Cl** complexes the COO^- group is coordinated to the nickel as a monodentate mode. Magnetic moment of the complex in DMSO is slightly higher than zero and the signals at ^{1}HNMR appeared in a normal range with fairly broadening corresponding to a d^8 diamagnetic configuration. Also, there is no band beyond 600 nm in the visible region of electronic spectra (Fig. 1a). Hence, structure of the complex is four-coordinate square planar (Fig. 2). In contrast to other complexes, electronic spectrum of the **Ni(HL^{COO})** complex in water is different from DMSO solution. So, a broad band in low energy region (>750 nm) confirms a six-coordinate octahedral geometry in water (Fig. 1b).

^{1}HNMR of diamagnetic **Zn(HL^{COO})** complex showed purity of complex and depicted clear evidences for deprotonation of carboxylic acid (COOH) and phenolic hydrogen (OH). After coordination of Zn(II) to the ligand. The peaks at 12.65 and 11.46 ppm correspond to COOH and OH, respectively, disappeared in the spectrum. Also, all of the aromatic and iminic protons' peaks shifted to higher fields. In the FT-IR spectrum of **Zn(HL^{COO})** complex similar to **Mn(HL^{COO})(OAc)** no band has seen above 1618 cm^{-1}. Thus, we think similar to **Mn(HL^{COO})(OAc)** complex the carboxylate group of the ligand is ionic in the complex. However, coordination of water molecules to form higher coordination numbers for zinc complexes is usual.

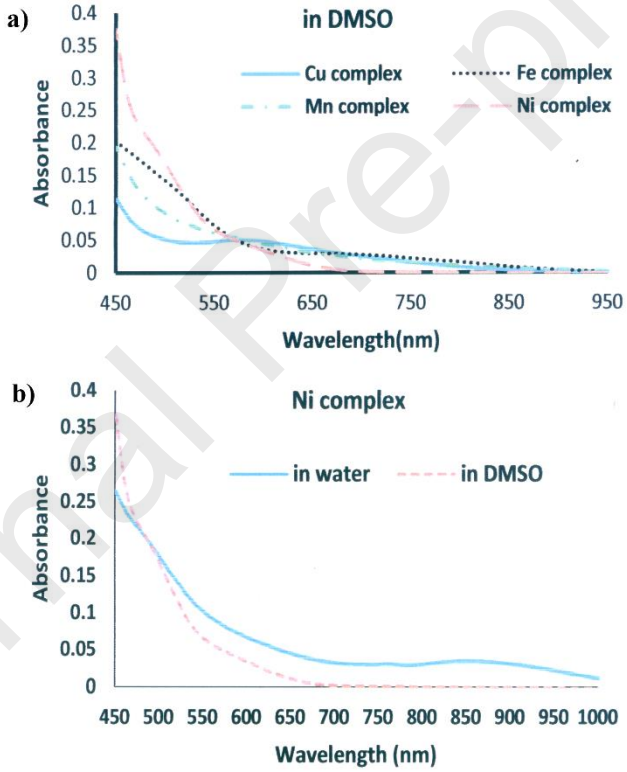

Fig. 1. a) visible spectra for **Mn(HL^{COO})(OAc)**, **Fe(HL^{COO})Cl**, **Ni(HL^{COO})** and **Cu(HL^{COO})** complexes in DMSO b) visible spectra for **Ni(HL^{COO})** complex in water and DMSO

.

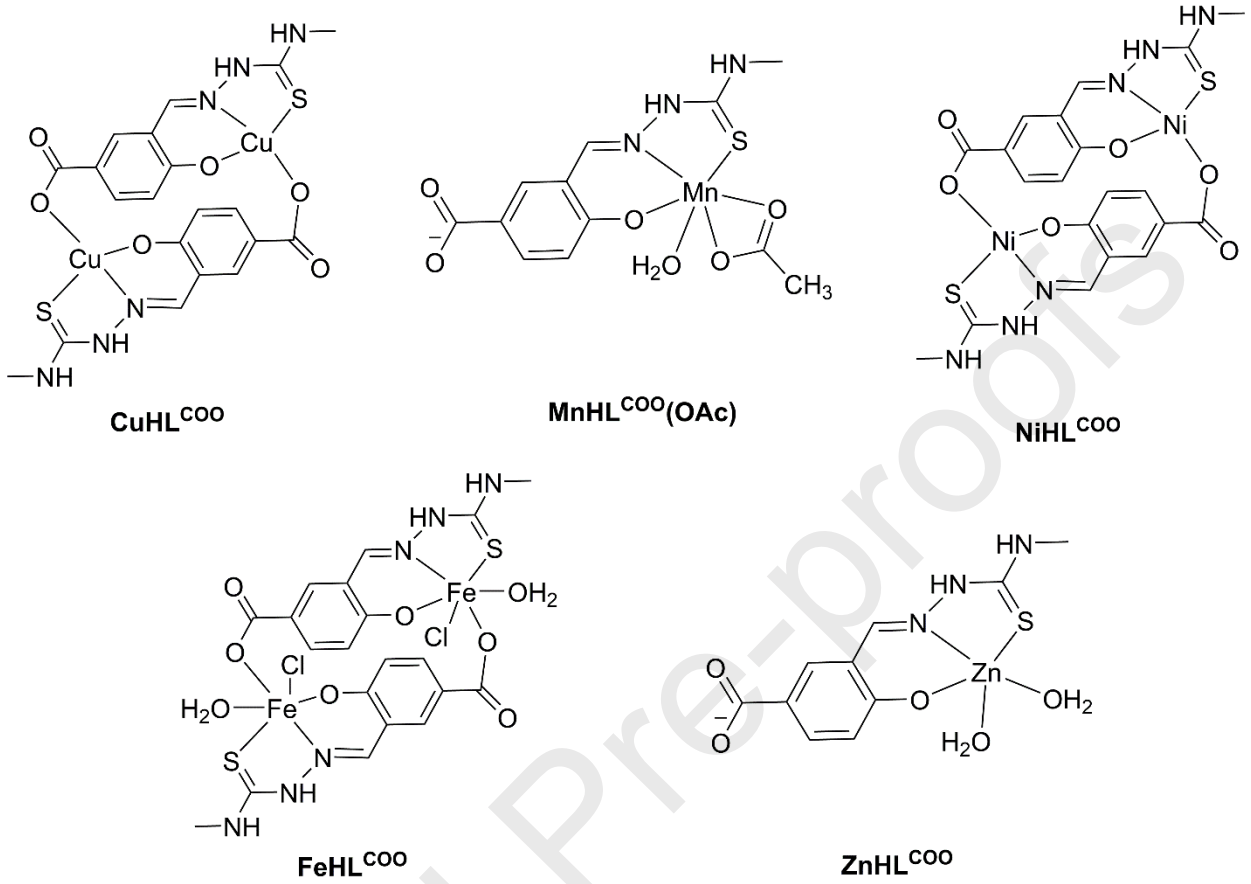

Fig. 2. Proposed structures for complexes

3.2. X-ray crystallography of the ligand

Crystal structure of the ligand $\mathbf{H_3L^{COOH}}$ is shown in Fig. 3 and main crystallographic data are summarized in Table 1 and angles and bond lengths in Table 2. The ligand crystallizes in the monoclinic space group $P2_1/n$ together with one acetonitrile molecule in the asymmetric unit. The thion form of the free ligand is supported by the C=S bond distance with a value of 1.693(4) Å and bond distance is in the range (1.686(3)-1.730(7) Å) found for similar ligands [27, 38, 39].

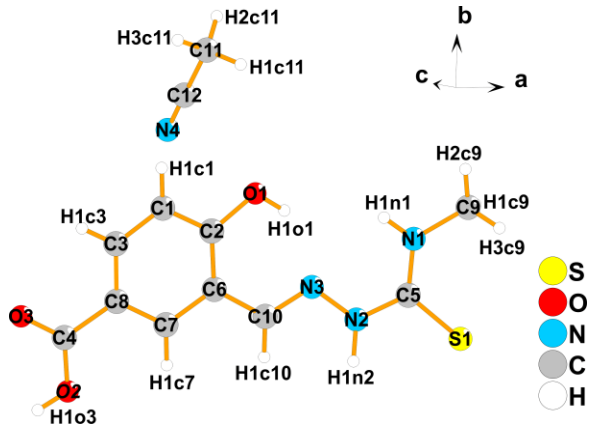

Fig. 3. Molecular structure of $\mathbf{H_3L^{COOH}}$

Table 1. Crystal data and structure refinement parameters for $\mathbf{H_3L^{COOH}}$

Empirical formula	$C_{12}H_{14}N_4O_3S_1$
Formula weight	294.3
Temperature/K	120.00(10)
Crystal system, Space group	Monoclinic, $P2_1/n$
a (Å)	4.8466 (6)
b (Å)	22.2692 (17)
c (Å)	12.664 (2)
β/°	91.630 (11)
Volume/Å^3	1366.3 (3)
Z	4
μ/mm^{-1}	2.24
F(000)	616
T_{min}, T_{max}	0.647, 1
Crystal size/mm^3	0.38 × 0.07 × 0.06
Radiation	Cu Kα
Measured reflections	3907
Independent reflections	3872
R_{int}	0.104
$R[F^2>3\sigma(F^2)]$	0.080
$wR(F^2)$	0.143
S	2.42

Table 2. Some selected bond lengths and angles for **H_3L^{COOH}**

Bonds lengths (Å)			
S1–C5	1.693(4)	N1–C5	1.312(6)
O1–C2	1.353(5)	N1–C9	1.471(5)
O1–H1o1	0.82(5)	N2–N3	1.382(4)
O2–C4	1.303(5)	N2–C5	1.359(5)
O2–H1o3	0.86(5)	N3–C10	1.294(5)
O3–C4	1.240(5)	N4–C12	1.120(7)
Bond angles (º)			
C2—O1—H1o1	111(3)	S1—C5—N1	124.1(3)
C4—O2—H1o3	109(3)	S1—C5—N2	117.8(3)
N2—N3—C10	113.7(3)	N1—C5—N2	117.9(4)
N3—C10—C6	121.3(4)	N3—C10—H1c10	119.36

The packing of this compound is governed by the combination of H-bonding (Table 3) and a typical π-π stacking along *a* axis. H-bonding creates an infinite zigzag chain of **H_3L^{COOH}** molecules connected through carboxylic acid (O2—H1O3···O3) and thioamide (N2—H1N2···S1) homodimers (see Fig. 4).

This chain is decorated with the acetonitrile molecules which are connected by partially accepting two H-bonds from the hydroxyl and second NH of the terminal thioamide of the **H_3L^{COOH}** molecule, with distances O1…N4 = 2.917(5) Å and N1…N4 = 2.988(6) Å. The hydroxyl hydrogen also participates in an intramolecular H-bond with the acceptor being the azido nitrogen. The neighbouring chains are connected by a non-classical CH-N bond between the acetonitrile methyl group and the carboxyl carbonyl of the ligand distance, with the distance C11…O3 being 3.269 (5) Å.

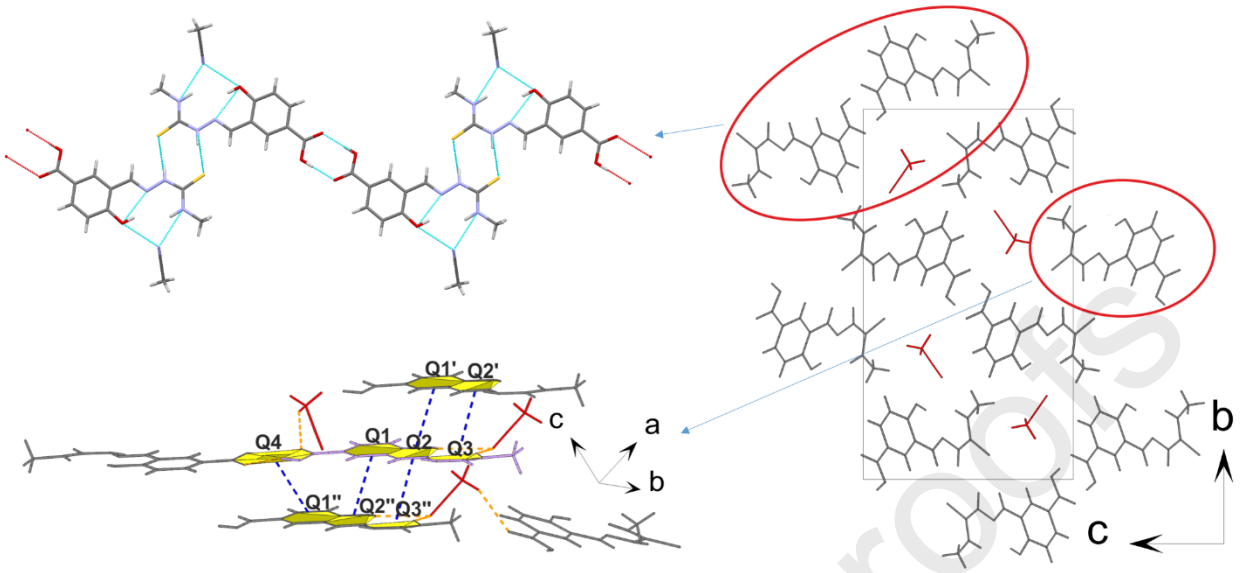

Fig. 4 Non-bonding interactions in the crystal structure $\mathbf{H_3L^{COOH}}$ acetonitrile solvate. Right – crystal packing with the two types of interactions highlighted, top left– H-bonding, bottom left– π-π stacking

The second most prominent feature of the structure is an atypical π-π stacking (Table 4). We can considered four different 'delocalization' rings inside the structure as the origin of the π-stacking: Q1 = C1-C2-C6-C7-C8-C3, Q2 = C2-O1-H1o1-N3-C10-C6, Q3 = N3-N2-C5-N1-H1N1 and Q4 = O3-C4-O2-H1o1-$O3^{i}$-$C4^{i}$-$O2^{i}$-$H1o1^{i}$ (with Symmetry codes i : -x, -y, -z+2). The distances of ≈ 3.5 Å and angles 95-110° (Table 4) are similar to common π-π stacking between phenyl rings [43-45].

Table 3. Selected hydrogen bonding interactions in the structure of $\mathbf{H_3L^{COOH}}$

D–H···A	D–H	H···A	D···A	D–H···A
O1—H1O1···N3 intra	0.83(5)	2.00(5)	2.701(4)	143(4)
O2—H1O3···$O3^{i}$	0.86 (5)	1.78 (5)	2.619 (4)	166 (4)
N2—H1N2···$S1^{ii}$	0.97 (5)	2.38 (5)	3.323 (4)	165 (3)
C11—H2C11···$O3^{iii}$	0.96	2.43	3.269(5)	145
O1—H1O1···$N4^{iv}$	0.83(5)	2.60(5)	2.917(5)	104(4)
N1—H1N1···$N4^{iv}$	0.95 (4)	2.19 (5)	2.988 (6)	141(4)

Symmetry codes: (i) −x, −y, −z+2; (ii) −x+3, −y, −z+1; (iii) x+1/2, −y+1/2, z−1/2; (iv) x+1, y, z.

Table 4. π-π non-bonding interactions in $\mathbf{H_3L^{COOH}}$

Dummy atom A	Dummy atom B	Dummy atom C	Distances A…B(Å)	Angles (A…B…C)°
Q1	Q2''	Q1''	3.5380(4)	110.024(4)
Q4	Q1''	Q2''	3.5330(3)	104.401(3)
Q2	Q3''	Q2''	3.5421(5)	97.635(3)

3.3. Lipophilicity of the compounds

Lipophilicity is one of the most important factors that illustrates the molecule's ability to pass through cell membranes [46]. The lipophilicity of the compounds was quantified by calculating the concentration ratio of the compounds in water and 1-octanol. All compounds were mostly distributed in the aqueous phase after mixing. The results indicate that these compounds have very low lipophilicity. Therefore, we can expect, that any possible cytotoxicity of the compounds would not be related to their high level of lipophilicity.

3.4. Stability determination

When working with Schiff bases and their complexes, we must consider sensibility of C=N bond to water and the following hydrolysis. Therefore, the stability of Schiff base ligand and their complexes in aqueous solution was followed by UV-Vis spectroscopy at acidic, basic and neutral conditions (pH = 1, 7.4 and 11) for 4 days in the range of 250–500 nm. Almost all compounds were stable up to 4 days in water at acidic, neutral and basic pHs (Fig. 5). All our further studies on the compounds took less than two hours and were performed in neutral media two days. Therefore, there was no problem with instability of these compounds in aqueous solutions.

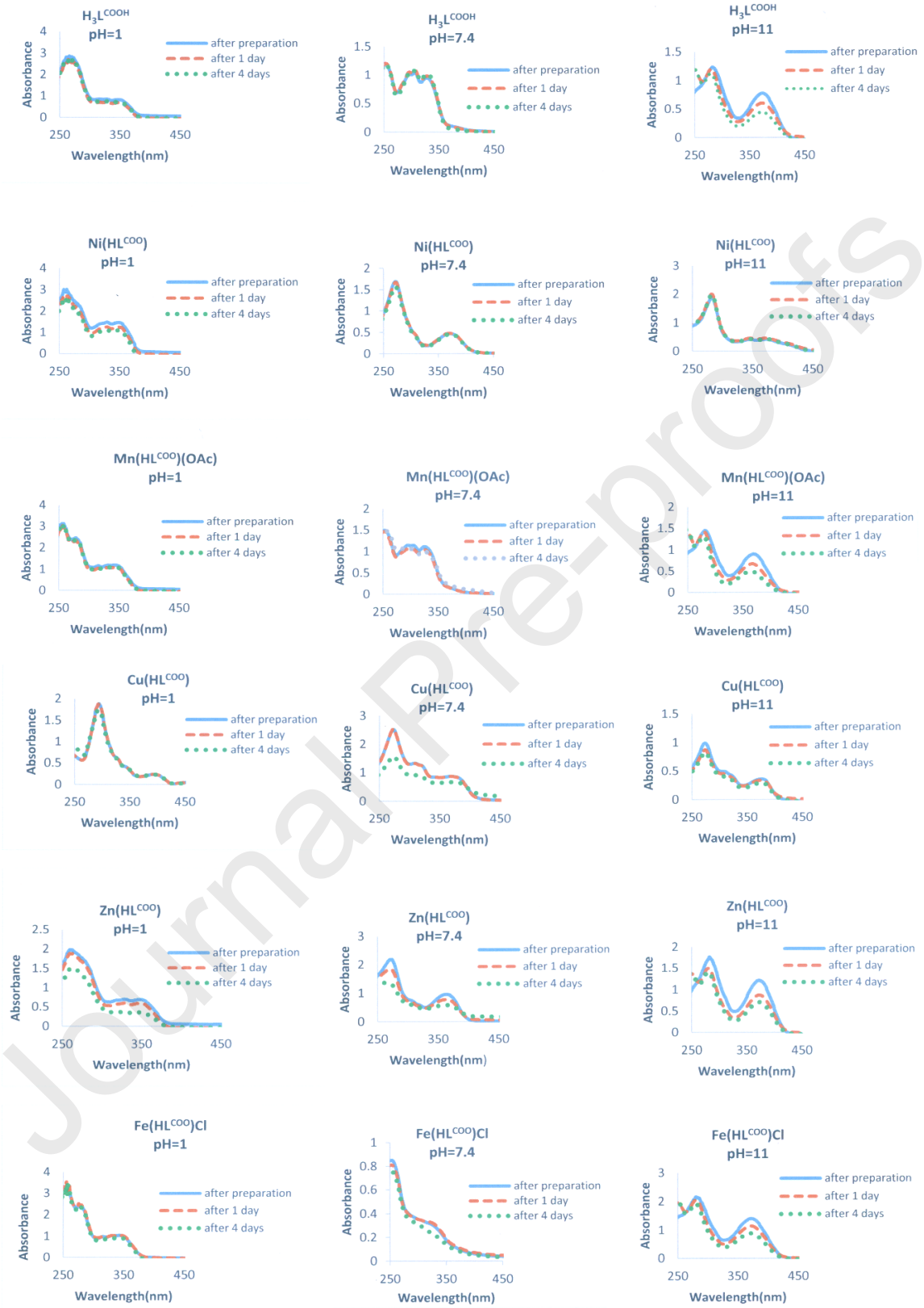

Fig. 5. Electronic absorption spectra for the ligand and complexes at different pH values.

3.5. Anticancer activity

3.5.1 Cell growth inhibition

MTT assay was used for determination of the cytotoxicity of the ligand and its complexes on MCF-7 and K562 cell lines. The outcome (shown in Table 5) were evaluated according to cell inhibition which are illustrated as IC_{50} values. The anti-proliferative activity of the studied complexes was higher than the free ligand, which demonstrates that the chelation of metal ion is the reason of high cytotoxic character of the complexes. IC_{50} values for $\mathbf{H_3L^{COOH}}$ and its complexes (Table 5) are much lower than of our reported values for $H_2L^{SO_3^-}$ and its complexes [27] (Table 6). Thus, the new compounds have higher cytotoxicity on K562 cell line. The effect of the compounds on MCF-7 cell line is more time-dependent than on K562. For the majority of the compounds, except **Fe(HL^{COO})Cl**, the time (24 h to 48 h) had small effect on viability of the K562 cells. **Ni(HL^{COO})**, **Zn(HL^{COO})**, **Mn(HL^{COO})(OAc)** and **Fe(HL^{COO})Cl** are more effective against K562 cells and only $\mathbf{H_3L^{COOH}}$ is more effective on MCF-7 cells. The **Cu(HL^{COO})** complex exhibited the highest cytotoxicity against both cell lines, also this complex showed better activity than Taxol as a drug in breast cancerthrapy. Therefore this complex was selected for further studies.

Table 5. IC_{50} (µg/mL) values of the ligand and complexes for the selected cells at 24 and 48 h.

Compounds	**IC_{50} (µg/mL) on K562**		**IC_{50} (µg/mL) on MCF-7**	
	24 h	**48 h**	**24 h**	**48 h**
Ligand	>200	>200	107.3±5.86	69.00±2.07
Mn(HL^{COO})(OAc)	21.93±3.21	18.45±1.85	63.14±2.91	46.45±1.45
Fe(HL^{COO})Cl	82.82±3.45	22.48±3.34	101±3.23	57.4±2.08
Ni(HL^{COO})	18.14±2.36	17.18±1.08	77.5±1.45	29.72±0.76
Cu(HL^{COO})	13.9±2.09	10.19±0.17	12.95±1.04	12.85±0.93
Zn(HL^{COO})	33.95±2.98	27.68±2.06	89.15±2.09	37.59±1.03
Positive controls	0.27±0.15	0.13±0.05-	59.21±3.02	18.1±1.34

Table 6. IC_{50}(µg/mL) values and solubility of H_2L^{SO3-} and its complexes on K562 cell line.

compound	IC_{50} for 24h	IC_{50} for 48	Solubility (g/L)
$H_2L^{SO}{}_3$	—	—	50
$NiHL^{SO}{}_3$	> 150	> 150	50
$[Cu(HL^{SO}{}_3)]_2$	130	110	10
$ZnHL^{SO}{}_3$	130	110	50

3.5.2. Determination of cell death

3.5.2.1. Apoptosis detection using Hoechst staining technique

The changes in the nuclear morphology of the cells were investigated by utilizing fluorescent microscopy (a qualitative method). As shown in Fig. 6, the control cells (untreated cells) showed large and round form, while the cells after treatment with **Cu(HL^{COO})** complex exhibited chromatin condensation and fragmentation. The results demonstrated that the **Cu(HL^{COO})** complex induced apoptosis in K562 cells.

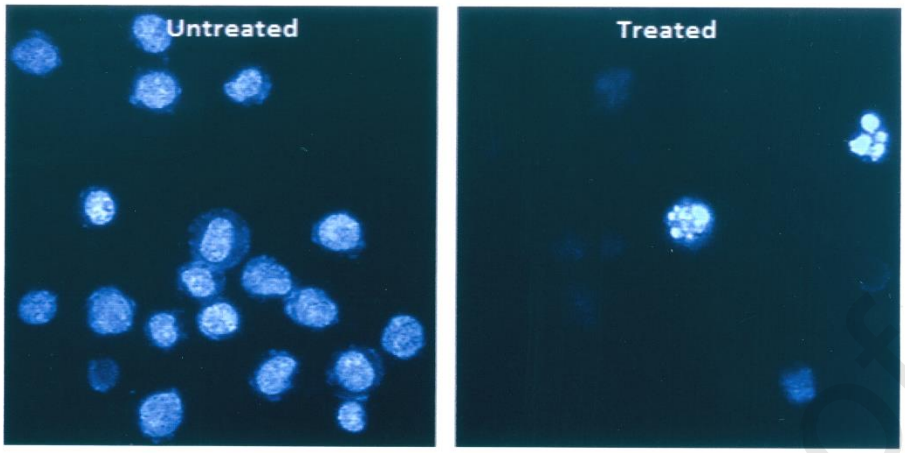

Fig. 6. Morphological study of the K562 cells treated with **Cu(HL^{COO})** (at IC_{50} value) after 48 h.

3.5.2.2. Evaluation of apoptosis by flow cytometry

A lot of cancer drugs based on metals apply their cytotoxic impact through apoptosis. Therefore, we used Annexin V/PI staining and flow cytometric method to determine whether the decrease in human tumour cell growth was attributable to the induction of apoptosis of cancer cells. This analysis quantifies the level of apoptosis. The obtained results indicated that K562 cells undergo apoptosis and not necrosis when they are treated for 24 h in the presence of **Cu(HL^{COO})**. In the control population of K562 cells, 99.5 % of cells remain alive as they stained negative for both annexin V-FITC and PI (lower left quadrant of Fig. 7a). However, after 24 h of **Cu(HL^{COO})** treatment (at IC_{25} value) 7.43% of cell populations doubled (upper right quadrant of Fig. 7b) illustrating that they are late apoptotic. There is a population of early apoptotic cells (23.7%) that are annexin V positive and PI negative (lower right quadrant of Fig. 7b). After morphological study, these data verified that cytotoxic effect of **Cu(HL^{COO})** is associated by induction of apoptosis and not necrosis.

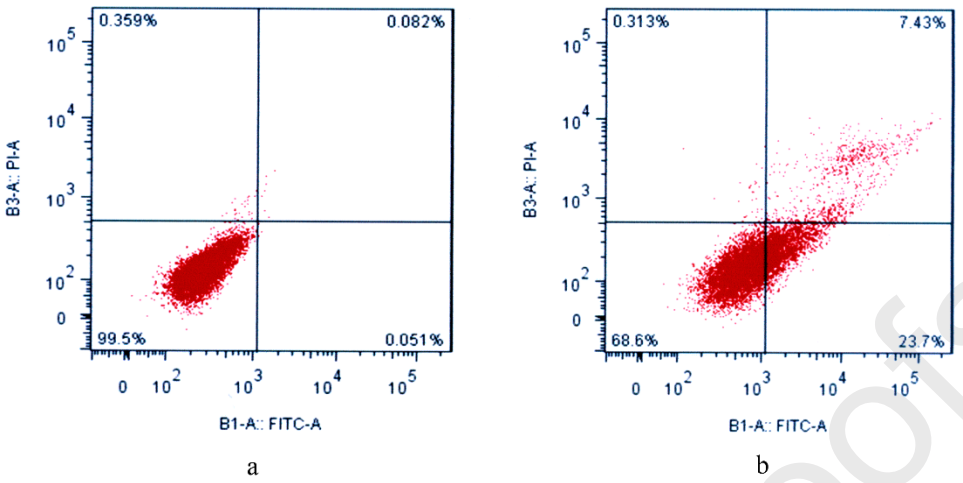

a b

Fig. 7. Quantitatively analysis of apoptosis in the K562 cells treated with IC25 value of the **Cu(HL^{COO})** complex was studied by annexin-V/PI double staining assay. The K562 cells treated with (a) and without (b) of the complex for 24 h and assessed by flow cytometry

3.5.2.3. Cell cycle analysis

Flow cytometry and PI staining analysis were performed to investigate the cell cycle phase distribution in **Cu(HL^{COO})** on the K562, after 24 and 48 hours of treatment. After treatment of the K562 cells with **Cu(HL^{COO})**, a significant increase in the sub-G1 cell (apoptotic cells) population was detected compared to the control cells that showed the strong evidence of inducing apoptosis (Fig. 8). An increase in G0/G1phase population after 48 h treatment indicates that **Cu(HL^{COO})** arrests cells in the G0/G1 phase. Percentage of untreated cells in the sub-G1, G0/G1, S and G2/M phases were computed 3.80%, 43.3%, 19.4% and 32.5%, respectively. While these proportion for the cells treated with **Cu(HL^{COO})** obtained 12.9%, 42.7%, 19.5%, 23.1% for 24 h and 24.0%, 50.0%, 18.1%, 6.58% for 48 h, respectively. Cisplatin inhibits cells predominantly in the S-phase that acts as a DNA covalent-binding agent to block DNA replication [47]. But our results revealed the mechanism of action of our compounds is different relative to cisplatin. Also the result of cell

cycle analysis revealed that **Cu(HL^{COO})** critically obstructed cell's growth in a time dependent condition.

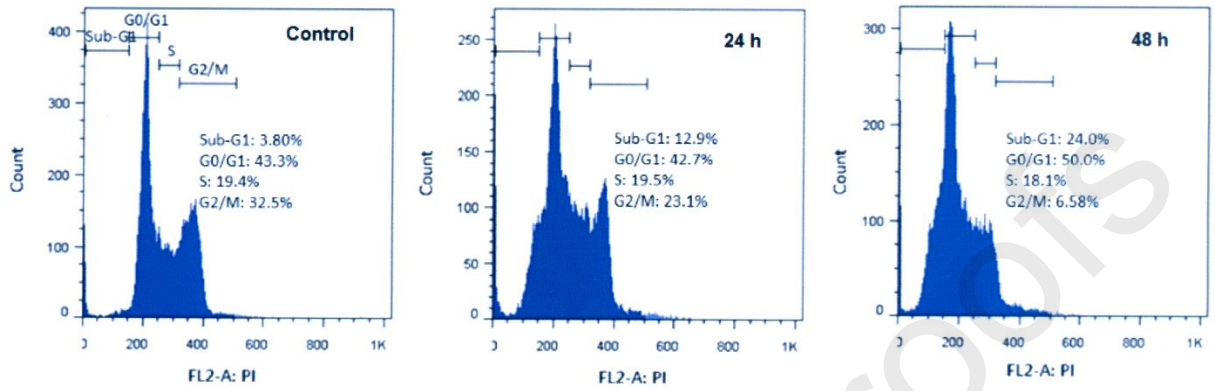

Fig. 8. Cell cycle analysis of the K562 cells treated with **Cu(HL^{COO})** complex after 24 –48 h. the percentage of the cells was determined in each phase of cell cycle by flow cytometry. The percent of K562 cells population in sub-G1 phase in untreated (control) and treated cells for 24 and 48 h were reported 3.80%, 12.9%, and 24.0%, respectively.

3.5.2.4. Intracellular ROS measurements

Some chemical compounds promote a sudden increase of ROS inside cells that lead to activation of apoptosis and promote cell death [48]. Therefore, probing the cellular ROS levels is important to understand mechanism of compound induced apoptosis. Fig. 9 indicated that K562 cells exhibited gradual increase in the ROS levels when treated with **Cu(HL^{COO})** complex at IC_{50} dose for 24 and 48 h compared with the control. Also there is a noteworthy time-dependent raise in DCF fluorescence (the cellular ROS levels) after 24-48 h treatment. These findings suggeste that this the antitumor activity of the complex can be due to its ability to generate cytotoxic ROS during a redox cycle.

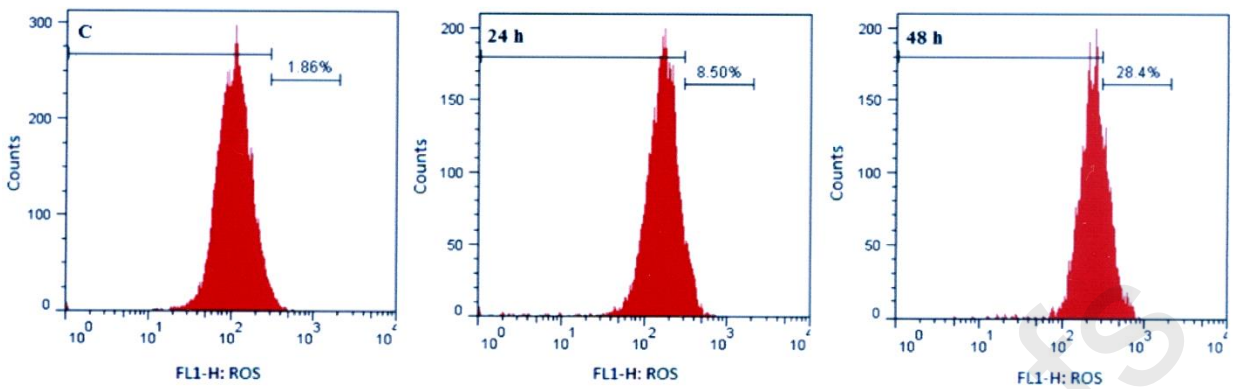

Fig. 9. Flow cytometry analysis of cellular ROS level in K562 cells treated by **Cu(HL^{COO})** complex. The K562 cells were treated with IC_{50} dose of the complex for 24-48 h. Then, cells were incubated with DCHF-DA and detected by flow-cytometry

4. Conclusion

Synthesis and characterization of new water-soluble thiosemicarbazone ligand and its complexes is presented. Their anticancer activity against two cell lines (K562 and MCF-7) were examined. In comparison with the free ligand, all complexes demonstrated significantly increased anticancer activity. Among the complexes, the **Cu(HL^{COO})** complex showed highest cytotoxicity on both cell lines. Investigation of the anticancer mechanism of action of the **Cu(HL^{COO})** complex confirmed that it is due to an increase in the apoptotic process. The results of flow cytometry analysis indicated that apoptosis of cancer cells induced by complex occurred via formation of ROS. Furthermore, analysis of cell cycle progression revealed that treatment of K562 cells with **Cu(HL^{COO})** resulted G0/G1 phase cell cycle arrest. These experimental results showed these new compounds with COOH functional group on the backbone of the ligand increased anticancer activity compared to similar compounds with SO_3^- functional group.

Acknowledgement

We would like to thank University of Tabriz–Iran for supporting this work. The crystallographic part was supported by the project 18-10504S of the Czech Science Foundation using instruments of the ASTRA laboratory established within the Operation program Prague Competitiveness - project CZ.2.16/3.1.00/24510.

Also we are so thankful to Sakha Pezhhanfar because of carefully reading the manuscript, editing it, and giving helpful coments.

Appendix A. Supplementary material

CCDC 1921450 contains the supplementary crystallographic data for H_3L^{COOH}. These data can be obtained free of charge from The Cambridge Crystallographic Data Centre via www.ccdc.cam.ac.uk/data_request/cif.

References

[1] J. Reedjik, Inorg. Chim. Acta 198 (1992) 873-881.

[2] J. Reedjik, Pure Appl. Chem. 59 (1987) 181-192.

[3] A. Terenzi, M. Fanelli, G. Ambrosi, S. Amatori, V. Fusi, L. Giorgi, V. T. Liveria, G.Barone, Dalton Trans. 41 (2012) 4389-4395.

[4] M. Frezza , S. Hindo , D. Chen, A. Davenport, S. Schmitt, D. Tomco, Q.P. Dou, Curr. Pharm. Des. 16 (2010) 1813-1825.

[5] G. Sathyaraj, T. Weyhermuller, B.U. Nair, Eur. J. Med. Chem. 45 (2010) 284-291.

[6] D.S. Raja, N. S. P. Bhuvanesh and K. Natarajan, Dalton Trans. 41 (2012) 4365-4377.

[7] C.W. Hsu, C.F. Kuo, S.M. Chuang, M.H. Hou, Biometals 26 (2013) 1-12.

[8] C.C. Garcia, B.N. Brousse, M.J. Carlucci, A.G. Moglioni, M.M. Alho, G.Y. Moltrasio, D. Accorso, N.B. Damonte, E.B. Damonte, Antivir. Res. 57 (2003) 161-170.

[9] D.K. Sau, R.J. Butcher, S. Chaudhuri, N. Saha, Mol. Cell. Biochem. 253 (2003) 21-29.

[10] A.P. Rebolledo, G.M. de Lima, L.N. Speziali, D.F. Maia, C.B. Pinheiro, J.D. Ardisson, M.E. Cortes, H. Beraldo, Appl. Organomet. Chem. 17 (2003) 945-951.

[11] N.C. Kasuga, K. Sekino, M. Ishikawa, A. Honda, Yokoyama, M. Nakano, S. Shimada, N. Koumo, C.K.J. Nomiya, Inorg. Biochem. 96 (2003) 298-305.

[12] Z. Afrasiabi, E. Sinn, J.N. Chen, Y.F. Ma, A.L. Rheingold, L.N. Zakharov, N. Rath, S. Padhye, Inorg. Chim. Acta 357 (2004) 271-279.

[13] Z. Afrasiabi, E. Sinn, S. Padhye, S. Dutta, C. Newton, C.E. Anson, A.K. Powell, J. Inorg. Biochem. 95 (2003) 306-315.

[14] D. Kovala-Demertzi, M.A. Demertzis, J.R. Miller, C.S. Frampton, J.P. Jasinski, D.X. West, J. Inorg. Biochem. 92 (2002) 137-140.

[15] J. Easmon, G. Purstinger, G. Heinisch, T. Roth, H.H. Fiebig, W. Holzer, W. Jager, M. Jenny, J.J. Hofmann, Med. Chem. 44 (2001) 2164-2171.

[16] A.G. Quiroga, J.M. Perez, I. Lopez-Solera, J.R. Masaguer, A. Luque, P. Roman, A. Edwards, C. Alonso, C.J. Navarro-Ranninger, Med. Chem. 41 (1998) 1399-1405.

[17] I. Dilovic, M. Rubcic, V. Vrdoljak, S.K.J. Pavelic, M. Kralj, I. Piantanidab, M. Cindric, Bioorg. Med. Chem. 16 (2008) 5189-5198.

[18] G.Y. Lui, Z. Kovacevic, V. Richardson, A.M. Merlot, D.S. Kalinowski, D.R. Richardson, Oncotarget 6 (2015) 18748-18779.

[19] E. Gumienna-Kontecka, M. Pyrkosz-Bulska, A. Szebesczyk, M. Ostrowska, Curr. Med. Chem. 21 (2014) 3741-3767.

[20] D.J. Lane, T.M. Mills, N.H. Shafie, A.M. Merlot, R. Saleh Moussa, D.S. Kalinowski, Z. Kovacevic, D.R. Richardson, Biochim. Biophys. Acta 1845 (2014) 166-181.

[21] D.R. Richardson, P.C. Sharpe, D.B. Lovejoy, D. Senaratne, D.S. Kalinowski, M. Islam, P.V. Bernhardt, J. Med. Chem. 49 (2006) 6510-6521.

[22] Y. Yu, D.S. Kalinowski, Z. Kovacevic, A.R. Siafakas, P.J. Jansson, C. Stefani, D.B. Lovejoy, P.C. Sharp, P.V. Bernhardt, D.R. Richardson, J. Med. Chem. 52 (2009) 5271-5294.

[23] D.S. Kalinowski, D.R. Richardson, Pharmacol. Rev. 57 (2005) 547-583.

[24] H. Huang, Q. Chen, X. Ku, L. Meng, L. Lin, X. Wang, C. Zhu, Y. Wang, Z. Chen, M. Li, H. Jiang, K. Chen, J. Ding, H. Liu, J. Med. Chem. 53 (2010) 3048-3064.

[25] F. Bacher, E.A. Enyedy, N.V. Nagy, A. Rockenbauer, G.M. Bognar, R. Trondle, M.S. Novak, E. Klapproth, T. Kiss, V.B. Arion, Inorg. Chem. 52 (2013) 8895-8908.

[26] P. Kalck, F. Montell, Adv. Organomet. Chem. 34 (1992) 219-284.

[27] S.A. Hosseini-Yazdi, A. Mirzaahmadi, A.A. Khandar, M. Mahdavi, A. Rahimian, V. Eigner, M. Dusek, G. Zarini, J. Molecular Liquids 248 (2017) 658-667.

[28] D. F. Evans, J. Chem. Soc. (1959) 2003-2005.

[29] R.M. Irfan, D. Jiang, Z. Sun, D. Lu, P. Du, Dalton Trans. 45 (2016) 12897-12905.

[30] Computer program: CrysAlis PRO 1.171.38.43, Rigaku OD (2015).

[31] L. Palatinus, G. Chapuis, J. Appl. Cryst. 40(2007) 786-790.

[32] V. Petricek, M. Dusek, L. Palatinus, Z. Kristallogr. 229 (2014) 345-352.

[33] A. Albert, The Physico-Chemical Basis of Therapy: Selective Toxicity. Chapman and Hall, London 1979.

[34] F. Denizot, R. Lang, J. Immunol. Methods 89 (1986) 271-277.

[35] M. Ghasemian, M. Mahdavi, P. Zare, M. Ali Hosseinpour Feizi, J. Toxicol. Sci. 40 (2015) 115–126.

[36] T. Andrienko, P. Pasdois, A. Rossbach, A. P. Halestrap, PLoS One 11 (2016) e167300.

[37] P. J. Jansson, P. C. Sharpe, P. V. Bernhardt, D. R. Richardson, J. Med. Chem. 53 (2010) 5759-5769.

[38] S. A. Hosseini-Yazdi, A. Mirzaahmadi, A. A. Khandar, V. Eigner, M. Dušek, M. Mahdavi, S. Soltani, F. Lotfipour, J. White, Polyhedron 124 (2017) 156-165.

[39] S. A. Hosseini-Yazdi, A. Mirzaahmadi, A. A. Khandar, V. Eigner, M. Dušek, F. Lotfipour, M. Mahdavi, S. Soltani, Gh. Dehghan. Inorg. Chim. Acta 458 (2017) 171-180.

[40] G. B. Deacon, R. J. Phillips, coord. Chem. Rev. 33 (1980) 227-250.

[41] Lever, A. B. P. Inorganic Electronic Spectroscopy, 2nd Edition, Amsterdam, 1984.

[42] Geary, W. J. Coord. Chem. Rev. 1971, 7, 81-122.

[43] C.A. Hunter, K.R. Lawson, J. Perkins, C.J. Urch, J. Chem. Soc. Perkin Trans. 2 (2001) 651–669.

[44] C.R. Martinez, B.L. Iverson, Chem. Sci. 3 (2012) 2191–2201.

[45] M. Swart, T. Wijst, C.F. Guerra, F.M. Bickelhaupt, J. Mol. Model 13 (2007) 1245–1257.

[46] L. Fetzer, B. Boff, M. Ali, X. Meng, JP. Collin, C. Sirlin, C. Gaiddon, M. Pfeffer. Dalton Trans. 40 (2011) 8869–8878.

[47] J.-L. Qin, Q.-P. Qin, Z.-Z. Wei, C.-C. Yu, T. Meng, C.-X. Wu, Y.L. Liang, H. Liang, Z.-F. Chen, Eur. J. Med. Chem. 124 (2016) 417−427.

[48] M. Redza-Dutordoira and D.A. Averill-Bates, Biochim. Biophys. Acta-Molecular Cell Research 1863 (2016) 2977-2992.

Synthesis and characterization of a new water-soluble thiosemicarbazone ligand and also coordination behavior of this ligand towards Ni^{II}, Cu^{II}, Zn^{II}, Mn^{III} and Fe^{III} were reported. Anticancer activity of these compounds against two cell lines was investigated in depth.